MODELLING OF VENTILATED HYDROGEN DISPERSION IN PRESENCE OF CO-FLOW AND COUNTER-FLOW

S.G. Giannissi[1], I.C. Tolias[1], H. Ebne Abbasi[2], D. Makarov[2], J. Grune[3], K. Sempert[3]
[1] Environmental Research Laboratory, National Center for Scientific Research Demokritos, Aghia Paraskevi, Athens, 15341, Greece, sgiannissi@ipta.demokritos.gr
[2] HySAFER Centre, University of Ulster, Newtownabbey BT37 0QB, UK
[3] Pro-Science GmbH, Parkstrasse 9, Ettlingen, 76275, Germany

ABSTRACT

In the framework of the EU-funded project, HyTunnel-CS, an inter-comparison among partners CFD simulations has been carried out. The simulations are based on experiments conducted within the project by Pro-Science and involve hydrogen release inside a safety vessel testing different ventilation configurations. The different ventilation configurations that were tested are co-flow, counter-flow and cross-flow. In the current study, co-flow and counter-flow tests along with the no ventilation test ($\dot{m} = 5\ g/s,\ \mathrm{d} = 4$ mm) are simulated with the aim to validate available and well-known CFD codes against such applications and to provide recommendations on modeling strategies. Special focus is given on modeling the velocity field produced by the fan during the experiments. The computational results are compared with the experimental results and a discussion follows regarding the efficiency of each ventilation configuration.

Keywords: ventilation, fan, velocity field, mixing, turbulence, safety, LFL

1.0 INTRODUCTION

With the emerging hydrogen technology in transportation sector regulation, standards and codes should be reevaluated and renewed, in order to include safety aspects related to hydrogen–power vehicles. Special focus should be given on underground and confined spaces, such as tunnels and underground parking lots. Towards that direction aims the EU-funded project, HyTunnel-CS, which is a pre-normative research for safety of hydrogen driven vehicles and transport through tunnels and similar confined facilities.

Among HyTunnel-CS research activities is the study of mechanical ventilation efficiency as a mitigation measure in case of accidental hydrogen leak in closed space. For this purpose several experiments were performed with different release rates and nozzle diameters examining different ventilation configurations and intensities. Co-flow, counter-flow and cross-flow experiments with different wind speeds, including the no-ventilation case as reference case, were performed, in order to assess their efficiency. For the ventilation an axial fan is used with maximum flow velocity 8.8 m/s. The experiments were conducted by Pro-Science (PS) in 2019. Details on the experimental set-up and the entire experimental series can be found in [1].

In the present work, selective trials of PS experimental series are simulated by two project partners: National Center for Scientific Research “Demokritos” (NCSRD) and University of Ulster (UU). Each partner uses different CFD code and modeling strategy and an inter-comparison among partners’ simulations is carried out with the aim to validate the codes, evaluate each modeling approach and provide recommendations for CFD simulations in similar applications.

For the inter-comparison among simulations, the co-flow and counter-flow configuration and the case with no ventilation are simulated. The release takes place through a 4 mm nozzle with steady state mass flow rate 5 g/s and ventilation speed 5 m/s. The measurements indicated a stagnant pressure approximately equal to 11 bar just upstream the nozzle. Temperature measurements on the nozzle exit were not available.

The jet release was modeled using the notional nozzle concept. Based on the notional nozzle concept the under-expanded jet that is formed downwind the nozzle is not modeled explicitly using the CFD methodology. Instead the CFD dispersion starts from the region (the so-called notional nozzle) where

the pressure is settled down to ambient. The conditions at this fictitious location are calculated using various methods based on the different available approaches. A review and evaluation on some of the available notional approaches can be found in [2], while other approaches have been developed and presented in [3]-[5]. Each partner used a different notional nozzle approach.

Special focus was given on the modeling of the airflow field generated by the fan. Modeling of fan flow is a challenging task, because the fan can create swirling flow, can generate high turbulence levels and non-uniform velocity field across cross section. Domkundwar et al. [6] observed turbulence intensity as high as 50% for swirling jets in the region close to the swirler. Further downstream the intensity was substantially decreased. In [7], a 23% turbulent intensity was calculated for circular fan while even higher (33%) for box fan. Experimental data about turbulence were not available in PS tests. However, velocity measurements downstream the nozzle at different distance horizontally and laterally during the experiments indicated a slight non-uniformity of the average airflow velocity.

The next Sections provide the experimental description, the description of each modeling strategy, the inter-comparison of the simulations with the experiment, discussion on the results and finally the main concluding remarks.

2.0 PRO-SCIENCE EXPERIMENTAL DESCRIPTION

The experiments were performed by Pro-Science [1] inside a safety vessel, as shown in Figure 1. The safety vessel has an inner diameter of 6 m and a height of 8 m with total volume of 220 m^3. The vessel is equipped with numbers of vents, ports and windows for optical access, but during the unignited release experiments all openings except for the two large flanges (see Figure 1) were sealed. The two flanges that were open during the experiment have an inner diameter of 1890 mm and they are parallel and close to the ground. The propeller fan for mechanical ventilation was placed in one of the vent, while the other vent was kept open.

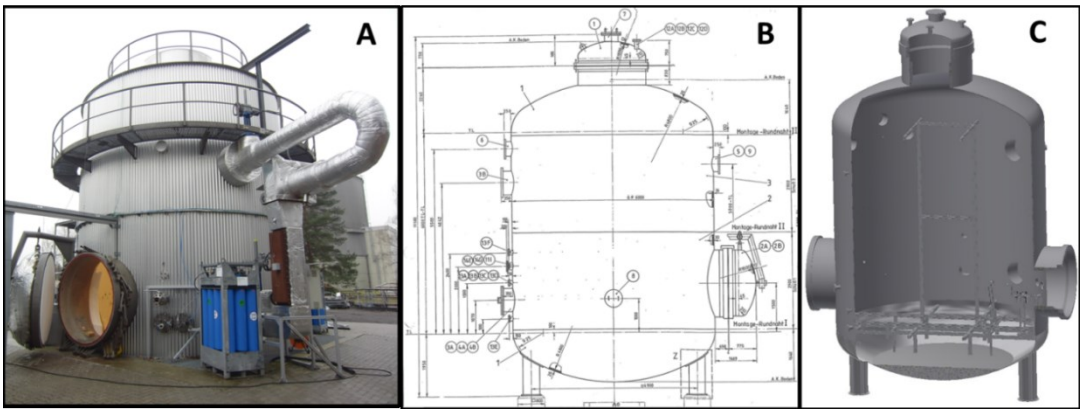

Figure 1. The experimental facility [8], photograph (left), technical drawing (center), CAD-drawing (right).

The H2 mass flow rate was adjusted and controlled by a Coriolis H2 Flow Meter (ELITE - Emerson Process Management). The flow runs through a bypass line which is equipped with the same nozzle as the intended jet release nozzle. After a stable flow was established through the bypass line, the bypass valve closed and the jet release valve opened simultaneously. The parameters that were measured were the nozzle diameter, mass flow rate and the pressure P2 (Kistler 40058F250) close to the release nozzle. Additionally, the pressure P1 (WIKA S 20) between the bypass valve and the release valve was recorded with a sample rate of 2 Hz.

The release nozzle is located above the release valve to avoid disturbance of the airflow from the ventilation in the co-flow configuration. The center axis of the jet is placed centered and perpendicular to the two large flanges of the vessel, in the co- and counter-flow configuration.

For the ventilation a wind machine (Trotec) TTW 20000 with a maximum air flow rate of 20000 m^3/h and a maximum air flow velocity of 8.8 m/s was used. The measured propeller diameter was 920 mm. The velocity profile produced by the fan was monitored with the help of sensors that were placed at different locations along the jet centerline x-axis and the lateral y-axis. Based on the measurements the airflow velocity exhibited a slight non-uniformity.

Two nozzle diameters (1 mm and 4 mm), two mass flow rates (1 g/s and 5 g/s) and four different airflow velocities (0 m/s, 1.5 m/s, 3.5 m/s and 5 m/s) were examined for the three investigated flow directions (co- , counter- and cross-flow).

In the present work, the test cases with 4 mm nozzle, 5 g/s mass flow rate with 0 m/s and 5 m/s airflow velocity for the co-flow and counter-flow configuration were chosen for simulation.

3.0 MODELLING DESCRIPTION

Two HyTunnel-CS partners participate in this study, NCSRD and UU. Each partner has the option to use a CFD code of their choice and to select the modeling strategy that will follow. In the next Sub-sections the modeling strategy of each partner on simulating the high-pressure jet release and the ventilation airflow field is presented.

3.1 NCSRD modeling strategy

The high-pressure jet release was modeled using the notional nozzle concept. The temperature at the actual nozzle was assumed equal to ambient. Birch 84 approach [9] was used to estimate the conditions at the notional nozzle, i.e. temperature equal to ambient and sonic velocity. The calculated notional diameter was 7.6 mm and the velocity 1275.9 m/s.

The notional conditions were set as H2 inlet conditions in the CFD dispersion modeling. The notional nozzle was set at the position of the actual nozzle and was modeled as a rectangular area with the same area as the notional one. Zero turbulence was set in the H2 inlet. However, simulations (for the no ventilation configuration) with 1% turbulence intensity at the inlet showed trivial impact on the results. This can be explained by the fact that the high released velocity into stagnant environment generates much higher turbulent kinetic energy than the initially relatively low imposed turbulence on source.

The most challenging task in simulating these experiments is the ventilation modeling. Generally, swirling flow and high turbulence can be generated by the fan. The swirling flow cannot be easily simulated. A simple approach to model flows generated by fans is to impose high turbulence in the inflow boundary. In the work, NCSRD modeled the fan airflow field using the following approaches:

1. **Uniform velocity profile across airflow plane**: set uniform velocity in the entire airflow plane with boundary conditions given value for velocity, turbulent kinetic energy and dissipation rate. Turbulence intensity (TI) equal to 10% and 50% was examined. The turbulent kinetic energy is estimated by the formula, $k = 3/2 \cdot (u \cdot TI)^2$ [10]. The dissipation rate is calculated by, $\varepsilon = c_\mu^{3/4} k^{3/2} / \ell$, where $c_\mu = 0.09$ and ℓ is the turbulent length scale. The turbulent length scale is derived by ℓ [10] with L the propeller diameter. A case with L equal to the flange opening diameter was also tested for TI=50% to examine the effect of a smaller dissipation rate (epsilon) on the results.

2. **Gaussian velocity profile across fan plane**: the inflow plane was modelled as a solid wall with a hole equal to the flange opening. A cyclic area equal to the fan diameter (see Figure 2) is designed and the ventilation boundary conditions (BC) were set on that region by imposing uniform given value for velocity and turbulence characteristics. On the flange opening (Figure 2) zero gradient BC to all variable was applied, while wall boundaries were specified in the rest plane (wall in Figure 2). A simulation without release was first carried out to calculate the 3D steady state flow field generated by the fan. Gaussian velocity profile was established. The 3D steady state

simulation was set as initial and inflow boundary condition in the simulation with hydrogen release.

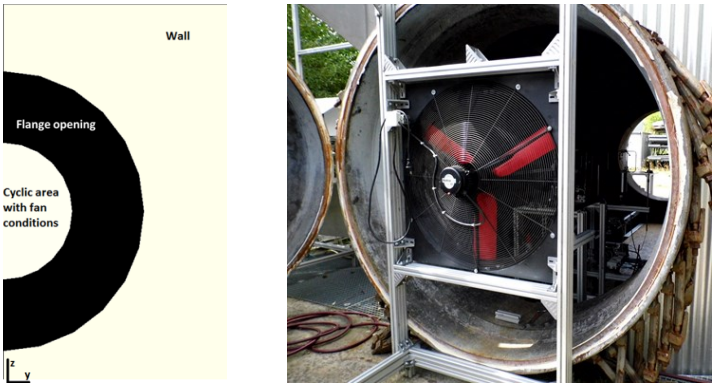

Figure 2. The design of airflow boundary (left) for the case "Gaussian velocity profile across fan plane". Symmetry along y-axis is assumed. A photograph from experimental facility showing the fan position (right).

The safety vessel was not modeled in both approaches as it is considered large enough to affect the jet. However, the fan inflow plane was set at a distance equal to the distance of the fan position from the nozzle in both co-flow and counter-flow, i.e. 2.6 m upwind and 4.776 m downwind the nozzle, respectively. In the no ventilation case, the domain was extended 5.5 cm upwind the release. Symmetry along y-axis was assumed in all cases. One cell was used to discretize the source area and small expansion ratios were used in the region close to the source. The maximum expansion ratio used was 1.12 further downwind the source. The total number of cells was 180 576, 153 504 and 168 402 for the no ventilation, co-flow and counter-flow configuration, respectively with the 1st approach (uniform profile). With the 2nd approach (Gaussian profile) the grid consists of 264 384 and 233 172 for co-flow and counter-flow configuration, respectively. Figure 3 shows the top and side view of the grid for the co-flow case with the 1st approach.

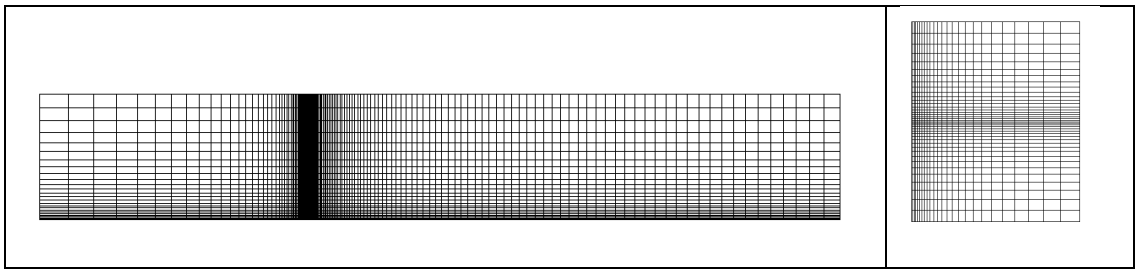

Figure 3. The grid on xy and yz plane for the co-flow simulation with the approach "uniform profile".

For the CFD dispersion the ADREA-HF code was used, which solves the 3D fully compressible conservation equations for the mixture and the hydrogen mass fraction conservation equation. Since, the jet was assumed to be released at ambient temperature no conservation equation for the energy was solved.

$$\frac{\partial \rho}{\partial t} + \frac{\partial \rho u_i}{\partial x_i} = 0 \tag{1}$$

$$\frac{\partial \rho u_i}{\partial t} + \frac{\partial \rho u_i u_j}{\partial x_j} = -\frac{\partial P}{\partial x_i} + \frac{\partial}{\partial x_j}\left((\mu + \mu_t)\left(\frac{\partial u_i}{\partial x_j} + \frac{\partial u_j}{\partial x_i} \right) \right) + \rho g_i \tag{2}$$

$$\frac{\partial \rho q_k}{\partial t} + \frac{\partial \rho u_j q_k}{\partial x_j} = \frac{\partial}{\partial x_j}\left(\left(\rho d_k + \frac{\mu_t}{Sc_t}\right)\frac{\partial q_k}{\partial x_j}\right) \quad (3)$$

where ρ-mixture density, kg/m^3; u – velocity, m/s; P-pressure, Pa; μ, μ_t - laminar and turbulent viscosity respectively, kg/m/s; Sc_t- turbulent Schmidt number, dimensionless; d - molecular diffusivity, m^2/s; q - mass fraction. The subscripts i, j denote the Cartesian i and j coordinate, respectively, index k denotes the component k.

For the turbulence, the standard k-epsilon model was employed with extra buoyancy terms [11]. The turbulence Schmidt number was set equal to 0.72.

Higher order numerical scheme was used for the convective terms (MUSCL scheme) and the central differences for the diffusive terms. For time integration the 1st order scheme was used. Small time step of 10^{-5} magnitude is adapted using a CFL restriction.

All boundaries except the symmetry plane and the airflow plane were considered open. A constant pressure boundary conditions (BC) was imposed at all the open boundaries except for bottom boundary where zero gradient BC was set at velocities. For the hydrogen mass fraction, zero gradient BC if outflow occurred and given value if inflow was specified.

3.2 UU modeling strategy

UU uses the ANSYS Fluent 2020R1 CFD code for the calculations. The governing equations include steady state mass-, momentum-, energy and species conservation equations based on the following formula:

$$\frac{\partial}{\partial x_j}\left(\bar{\rho}\tilde{u}_j\right) = 0 \quad (4)$$

$$\frac{\partial}{\partial x_j}\left(\bar{\rho}\tilde{u}_j\tilde{u}_i\right) = -\frac{\partial \bar{p}}{\partial x_i} + \frac{\partial}{\partial x_j}(\mu + \mu_t)\left(\frac{\partial \tilde{u}_i}{\partial x_j} + \frac{\partial \tilde{u}_j}{\partial x_i} - \frac{2}{3}\frac{\partial \tilde{u}_k}{\partial x_k}\delta_{ij}\right) + \bar{\rho}g_i \quad (5)$$

$$\frac{\partial}{\partial x_j}\left(\bar{\rho}\tilde{u}_j\left(\bar{\rho}\tilde{E} + \bar{p}\right)\right) =$$

$$= \frac{\partial}{\partial x_j}\left(\left(k + \frac{\mu_t c_p}{Pr_t}\right)\frac{\partial \tilde{T}}{\partial x_j} - \sum_m \tilde{h}_m\left(-\left(\bar{\rho}D + \frac{\mu_t}{Sc_t}\right)\frac{\partial \tilde{Y}_m}{\partial x_j}\right)\right) \quad (6)$$

$$\frac{\partial}{\partial x_j}\left(\bar{\rho}\tilde{u}_j\tilde{Y}_{H_2}\right) = \frac{\partial}{\partial x_j}\left(\left(\bar{\rho}D + \frac{\mu_t}{Sc_t}\right)\frac{\partial \tilde{Y}_{H_2}}{\partial x_j}\right) \quad (7)$$

$$\frac{\partial}{\partial x_j}\left(\bar{\rho}\tilde{u}_j\tilde{Y}_{O_2}\right) = \frac{\partial}{\partial x_j}\left(\left(\bar{\rho}D + \frac{\mu_t}{Sc_t}\right)\frac{\partial \tilde{Y}_{O_2}}{\partial x_j}\right) \quad (8)$$

where x_i,x_j,x_k are Cartesian coordinates, m; u_i, u_j, u_k are velocity components, m/s; t is time, s; p is pressure, Pa; ρ is density, kg/m^3; g_i is gravity acceleration, kg/m^2; μ_t is turbulent dynamic viscosity, kg/m/s; δ_{ij} is Kronecker symbol, E is the total energy; T is the temperature, K; Y_{H2} is hydrogen mass fraction, Y_{O2} is oxygen mass fraction, c_p is specific heat at constant pressure, Sc_t is turbulent Schmidt number, Pr_t is turbulent Prandtl number, D is molecular diffusivity, m^2/s; m is index of chemical specie (species are: H_2, O_2, N_2). Symbol "overbar" stands for Reynolds averaged parameters and "tilde" for Favre averaged parameters.

Flow turbulence was modelled using standard k-ε turbulence model [12]. Turbulent Schmidt and Prandtl numbers were set equal to $Sc_t = 0.7$ and $Pr_t = 0.85$, respectively. The molecular diffusivity of hydrogen was defined following [13] as $D_{H_2-Air} = 6.6 \cdot 10^{-5}(T/273)^{1.75}$, which provided $D_{H_2} = 7.07 \cdot 10^{-5}$ at T=284 K.

Mixture laminar viscosity, specific heat and thermal conductivity were calculated using mass-weighted mixing law. Specific heats were approximated as piecewise polynomial functions of temperature.

Simulations were conducted using a steady-state formulation of the pressure-based coupled solver. MUSCL numerical scheme was used for discretization of all transported variables with the second-order approximation of pressure gradients.

Effective nozzle model (Molkov, 2012) was applied to define jet parameters at the hydrogen release. The calculations were performed using the model realisation at the e-Laboratory website (https://elab-prod.iket.kit.edu/integrated/jet_parameters/input). To match experimental mass flow rate 5 g/s through 4 mm nozzle with flow temperature close to the nozzle T=284 K (due to long piping and extensive instrumentation) the effective nozzle diameter should be d_{eff}=7.57 mm. In simulations, the nozzle was modelled as a square with the side 6.71 mm. Hydrogen velocity and temperature at the inflow were equal to those in the effective nozzle, i.e. u_{eff}=1283 m/s and T_{eff}=284.4 K, hydrogen mass fraction in the nozzle Y_{H2}=1.0 and oxygen mass fraction Y_{O2}=0.0. Turbulence intensity I=25% and turbulence length scale l=0.002 m were imposed as boundary conditions in the nozzle for k-ε turbulence model equations.
To model the flow generated by the fan two approaches were used:

1. Uniform velocity profile in open atmosphere

A rectangular calculation domain with sizes LxWxH=4.4x1.3x1.3 m was used. The domain extended 3.75 m downstream from the release nozzle and 0.65m upstream. The domain was discretized using structured hexahedral mesh 84x54x54 control volumes (CVs), total CV number 244 944. The release nozzle was resolved using 4x4 CVs.
For quiescent conditions, the ambient gauge pressure p=0 Pa was used as a boundary condition for momentum conservation equations on all surfaces representing the atmosphere. For co-flow and counter-flow simulations, the effect of the fan was simulated imposing pressure gradient 15 Pa to reach flow velocity 5 m/s at the corresponding inflow boundary (realised using "intake fan" boundary of ANSYS Fluent software). The turbulent intensity is assumed to be 50%. The turbulent length scale was assumed to be 0.2 m. It was calculated as the distance between two strokes of propeller blades with three blades,

$$TS = V_{max} / \left(3 \cdot \omega_{max} / 60\right) \cong 0.2\,\text{m} \qquad (9)$$

where ω_{max} = 915 rev/min and V_{max} = 8.8 m/s based on the characteristics of fan. At the boundaries with atmosphere, the temperature T=284 K was used as a condition for energy conservation equations, hydrogen mass fractions Y_{H2}=0.0 and oxygen mass fraction Y_{O2}=0.23 for species transport equations. Turbulence intensity 10^{-6} and length scale 10^{-6} m were used as boundaries for k-ε turbulence model equations to mimic quiescent atmosphere.

2. Linear source term in vessel geometry

For simulations with the effect of the vessel, the domain included the vessel itself (height 8.8m, diameter 5.95m), and the area around the vessel with a radius of 12.5 m. Area of the jet development with sizes *L*x*W*x*H*=4.25×0.70×0.70 m (3.75 m downflow from the release nozzle and 0.50 m upflow) was discretised using structured hexahedral mesh 82×52×52 CVs. The square release nozzle was discretised 4×4 CVs. Far from the jet development area, the vessel was meshed using tetrahedral mesh targeting a maximum CV size of 0.75m. The number of CVs in the vessel was 752,149. The area ambient to the vessel was discretised using tetrahedral CVs growing from 0.05 m close to hatch openings up to 2.0 m at the periphery. Total CV number in the calculation domain was 781,107 CVs. Cross-section of the numerical mesh with the vessel geometry is given in Figure 4, left:

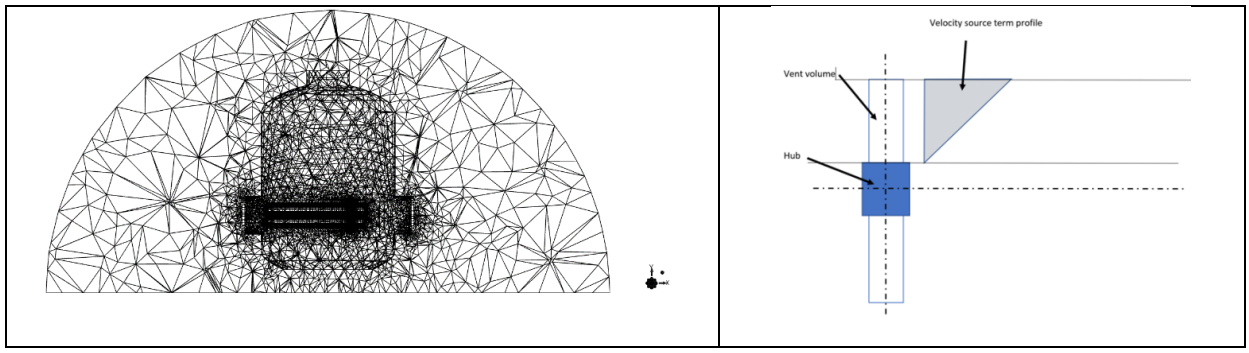

Figure 4. Cross-section of calculation domain with the experimental vessel (left) and a schematic diagram showing the linearly growing with radius value of the x-momentum source term (right).

To simulate co-flow and counter-flow the calculation domain had a specially designated area matching cross-section of the experimental fan and thickness 0.1 m (Figure 4, right). Effect of the fan for co-flow and counter-flow was simulated using volumetric source term for x-momentum conservation equation, which value was growing linearly with radius $S_u = 6201.6(R - R_{hub})$ N/m^3, where R is the radius from the fan centre and $R_{hub} = 0.133$ m is the radius of the fan hub. The source term value was obtained based on the specified maximum fan overpressure 110 Pa, the source term application area radius 0.46 m and thickness 0.1 m. It should be mentioned that for both aforementioned models (in open atmosphere and accounting effect of the vessel), the simulated fan induced velocity field is validated against available experimental data.

4.0 RESULTS AND DISCUSSION

Based on the experimental data [1] it was observed that co-flow and counter-flow configurations enhances the mixture mixing and leads to reduction of the LFL longitudinal distance compared to the case without ventilation (see also Figure 9). More precisely, the LFL distance in the case with no ventilation was 2.75 m, while for the co-flow and counter-flow it was reduced to 1.75 m and 2 m, respectively, i.e. the LFL distance was reduced by 36 % and 27 %, respectively. In the counter-flow an abrupt fall of concentration was observed at a distance 2.25 m downstream the nozzle due to the interaction of the jet with the ventilation airflow. Based on the experimental concentration contour plots on lateral plane (Figure 9, top) it was observed that co-flow ventilation reduced also the size of flammable mixture in lateral direction, whilst the counter-flow had the opposite effect.

Figure 5, left shows the volume fraction along the jet centerline for the no ventilation case. The results from applying the similarity law [4] for hydrogen concentration decay in open atmosphere are also shown in the same figure for reference. Good agreement is found among all simulations with a tendency by UU simulations to over predict the concentration further downwind the nozzle. The results by the two UU approaches, open atmosphere and vessel geometry, are almost identical with each other indicating that modelling the entire vessel does not affect the hydrogen distribution. Similarity law tends to over-predict the concentration at further distances and provides results in less agreement with experiment than CFD simulations.

Figure 5, right shows the radial profiles (with normalization) for the experiment, the NCSRD simulation and the UU simulation with vessel geometry at three distances from the nozzle, 125, 1000 and 2000 mm. The profiles are well predicted at all distances.

Figure 6 shows the simulation results for the co-flow case as predicted by the different approaches. The similarity law results are also shown for comparison. Two separate figures have been produced; in order the results to be distinguishable and easier to be compared. Figure 6, left shows the results with the main two approaches from each partner regarding the imposed airflow profiles across ventilation boundary, while Figure 6, right shows the NCSRD approaches for the uniform velocity profile approach comparing the results with different turbulent intensity levels and epsilon values. Satisfactory agreement is found among all predictions with a tendency to over predict the concentrations further downwind the nozzle. The approaches with uniform velocity profile by both

partners provide similar results. The Gaussian velocity profile approach gives also predictions very close to the uniform profile approaches. This occurs most likely due to the fact that in the jet core the flow characteristics are the same for both profiles. On the contrary, the prediction with the linear source term approach exhibits differences and is in better agreement with the experiment at the furthest distances (beyond 2 m). This is attributed to the different flow field used in this approach. The linear source term approach with zero velocity at the center generates gradients and high turbulence near the fan boundary. Turbulence is gradually decreased as we move away from the fan, as can be seen in Figure 10. Near the fan the turbulence kinetic energy is approximately equal to 9 m^2/s^2. Further downstream it reduced to less than 5 m^2/s^2. This observation supports the choice to use TI=50% (when TI=50% k is equal to 9.6 m^2/s^2) to the approaches with uniform velocity profile.

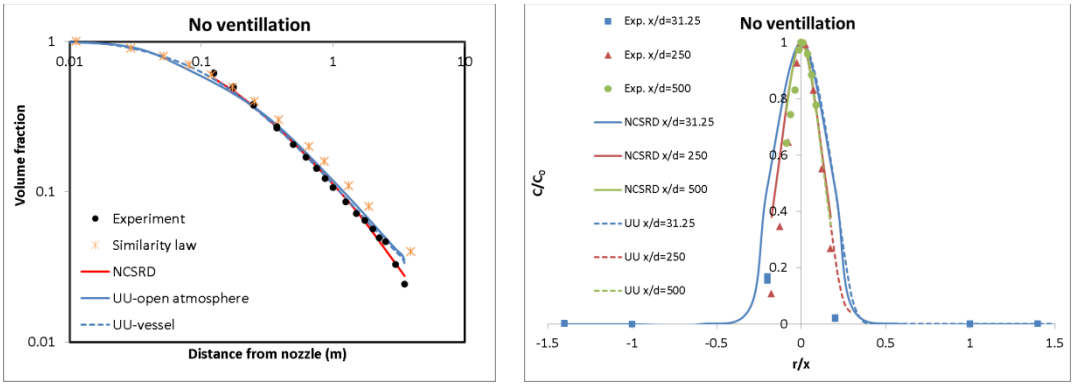

Figure 5. No ventilation: predicted and experimental volume fraction along jet centreline in log-log scale (left) and radial profiles (right). The results from similarity law are also shown.

Based on Figure 6, left when uniform velocity profile are imposed at the airflow boundary, high levels of turbulent intensity (TI=50 %) should be imposed to match better the measurements of the co-flow case. Smaller value for the dissipation rate (epsilon) leads also to better predictions. Generally, it was observed that the results are quite sensitive to turbulence characteristics. This indicates the significance to accurately predict the flow field generated by the fan.

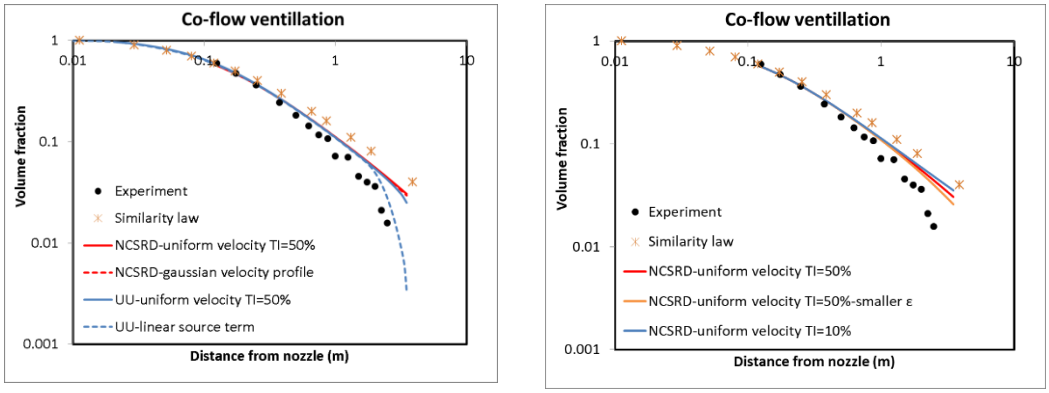

Figure 6. Co-flow configuration: predicted and experimental volume fraction along the jet centreline in log-log scale for the different velocity profiles (left) and for different turbulence characteristics (right).

Figure 7, left shows the radial profiles of the volume fraction for the co-flow configuration for the NCSRD-gaussian profile approach and the UU-linear source term approach for distances up to 2 m from the nozzle. The predicted profiles are similar with each other and in satisfactory agreement with the experiment. However, simulations tend to produce a slightly wider cloud at distances closer to the nozzle compared to the experiment.

Similarity law provides conservative results in the co-flow configuration, as it significantly over-predicts the concentration, especially at distances further downstream the nozzle.

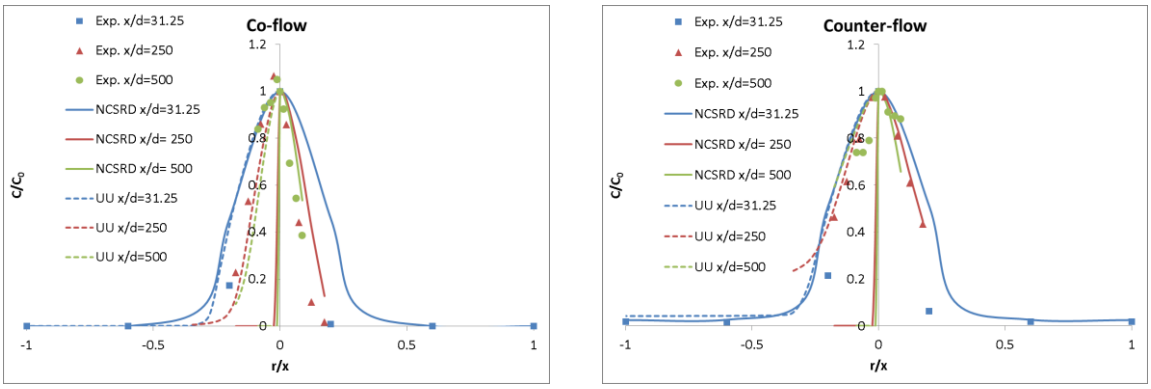

Figure 7. Radial profiles of volume fraction for the NCSRD-gaussian profile approach and the UU-linear source term approach at several distances from the nozzle for the co-flow (left) and the counter-flow (right).

Figure 8 shows the results for the counter-flow configuration in a similar way as in the co-flow. Good agreement is found for the distances close to the nozzle (up to 1.5 m), while deviations are found further downstream. More specifically, there are differences in the distance at which the jet interacts with the ventilation airflow, where the abrupt fall of concentration occurs. This distance is under estimated in all simulations with UU-uniform profile approach and NCSRD-uniform profile with TI=10% to have the least under prediction and match better the experimental results. When TI=50%, the NCSRD-gaussian profile approach gives better prediction than the NCSRD-uniform profile approach in terms of the distance of jet interaction with airflow. The authors believe that the reason for the differences between NCSRD and UU simulation results with uniform velocity profile and TI=50% could arise from different turbulence length scales, which, as suggested in [7], may have dominating effect on development of fan-generated flows. According to Halloran et al. [7], the turbulent length scale of the fan (and not the fan speed) dictates the turbulence. Another possible reason could be the different distance of the airflow boundary from the nozzle in the two simulations. Finally, at intermediate distances from the nozzle (0.8 m-1.5 m) the non-uniform velocity profile approaches tend to over-predict the concentration.

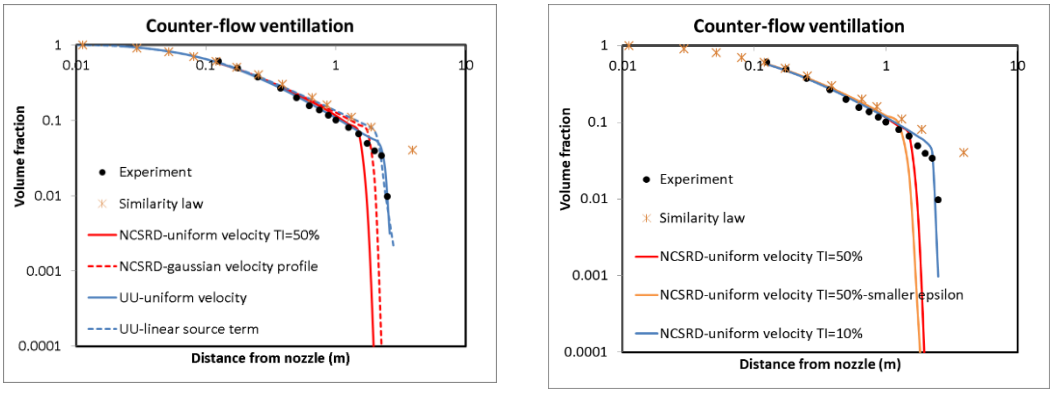

Figure 8. Counter-flow configuration: predicted and experimental volume fraction along the jet centreline in log-log scale for the different velocity profiles (left) and for different turbulence characteristics (right).

Similar to the co-flow configuration the results are sensitive to turbulence characteristics in counter-flow configuration as well. Contrast to co-flow, the NCSRD simulation with uniform velocity profile

and lower TI (TI=10%) provides better results than the counterpart with high TI. High turbulence seems to lead to less longitudinal jet spreading.

Figure 8, right shows the radial profiles for the counter-flow configuration for the NCSRD-gaussian profile approach and the UU-linear source term approach for distances up to 2 m from the nozzle. Similar remarks as in the co-flow configuration can be made.

Similarity law seems to over-predict the concentration in counter-flow configuration too. As expected, it deviates significantly at the distances further downwind the nozzle, as it does not account for the jet interaction with the fan flow.

Figure 9 displays the predicted and experimental contour plots for the concentration on xy plane for each configuration in comparison with the experiment. For the no ventilation, the simulations tend to slightly over-predict the distance of the lower flammability limit (LFL). The UU-vessel simulation and the NCSRD simulation over-predict the LFL distance only by 5% and 3%, respectively, whereas UU-open atmosphere gives an over-prediction by about 13 %. In the co-flow configuration, all simulations over-predict the LFL distance with the linear source term approach to have the least deviation (~26 %). The experimental trend to reduce the LFL distance by co-flow was also observed in the simulations with high turbulence. High turbulence leads to greater level of mixing and dilution of the mixture. In the counter-flow configuration, over-prediction of the LFL distance is observed by all UU simulations, while under prediction is observed in all NCSRD simulations except for the approach with Gaussian profile where there is a slight underestimation. The least deviation was found for the simulations with the linear source term and the Gaussian velocity profile (~5 % relative error). UU uniform profile approach follows close by.

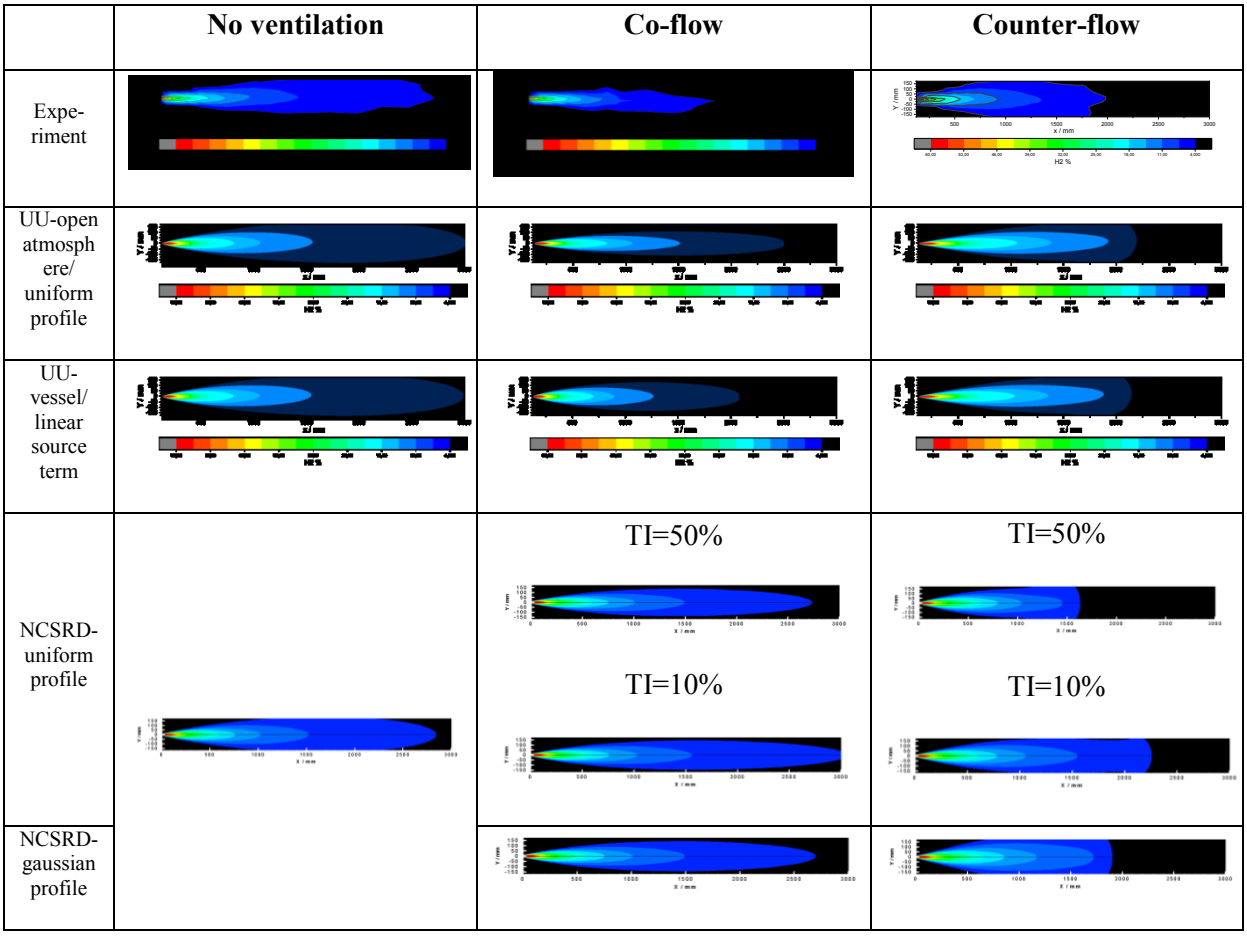

Figure 9. Concentration contour plot for the no ventilation (left), co-flow (center) and counter-flow (right) configuration. Same contour levels are used for all figures.

Finally, Figure 10 illustrates the turbulence kinetic energy contour plots on xy plane for the simulations with uniform velocity profile and non-uniform (linear and Gaussian) velocity profile by both partners. For NCSRD-uniform profile approach only the case with TI=50% is illustrated.

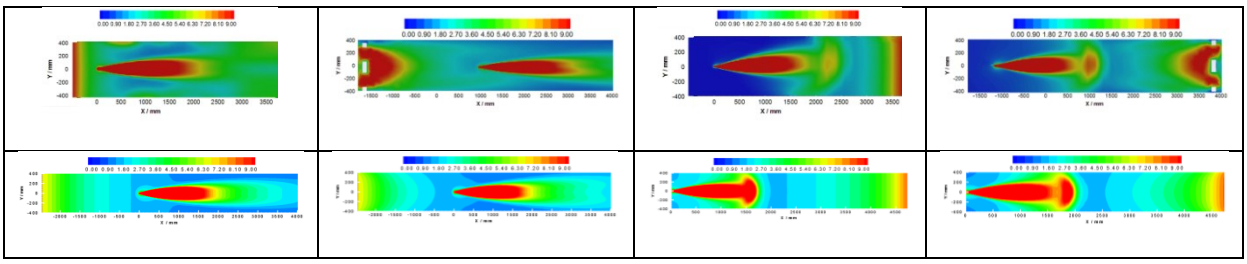

Figure 10. Turbulent kinetic energy contour plot. Top: UU simulations from left to right: co-flow uniform profile, co-flow linear source term, counter-flow uniform profile, counter-flow linear source term. Bottom: NCRD simulations from left to right: co-flow uniform profile, co-flow gaussian profile, counter-flow uniform profile, counter-flow gaussian profile.

5.0 CONCLUSIONS

An inter-comparison among CFD simulations was carried out within the HyTunnel-CS project and is presented here. Two partners participated in the study, NCSRD and UU, and simulated experiments performed by Pro-Science. The aim was two-fold: study the efficiency of mechanical ventilation in high-pressure hydrogen release inside an enclosure, such as parking or tunnel, and provide recommendations on modeling ventilated hydrogen dispersion.

The hydrogen release took place through a 4 mm nozzle with mass flow rate 5 g/s. Three different ventilation configurations were considered for this work, no ventilation, co-flow and counter-flow, with airflow velocity 5 m/s. Each partner used different modelling approaches and CFD codes for their simulations.

Special focus was given on the modelling of the flow generated by the fan and several approaches were tested. UU modelled the fan airflow by 1) imposing uniform velocity profile and TI=50% in open atmosphere and 2) imposing linear source term with zero velocities at the fan centre and include the entire vessel geometry. NCSRD modelled the fan airflow by 1) imposing uniform velocity profile and TI=50% and 2) imposing gaussian velocity profile. The vessel was not modelled in both NCSRD approaches. In the approach with uniform profile, different length scales (consequently epsilon values) and smaller TI (=10%) were also tested.

In the no ventilation configuration, the predictions were in good agreement with the experiment with UU simulations to over-predict the LFL distance. Comparison between the two UU simulations revealed that modelling the entire vessel within which the release takes place is not essential. The large volume of the vessel does not affect hydrogen dispersion.

Even though the vessel geometry does not influence the dispersion, the position of the ventilation boundary in the co-flow and counter-flow configuration can have an impact on results and thus it is recommended to be placed at a distance from the nozzle similar to the experiment.

In the co-flow configuration, the approach with linear source term mimics best the actual fan flow and gives the best agreement with the experiment. The rest approaches tend to over-predict the concentration at further distances downwind the nozzle. When uniform flow field is imposed at the fan boundary large values of turbulence intensity (50%) and small values of dissipation rate were required to improve the predictions, as they could model better the experimental flow conditions.

In counter-flow configuration, the approaches UU-uniform profile with TI=50% and NCSRD-uniform profile with TI=10% capture better the interaction of airflow with the jet. However, the linear source term approach and the gaussian velocity profile approach predict more accurately the LFL distance (over-prediction and under-prediction by 5%, respectively). Close follows the UU-uniform profile.

The NCSRD-uniform profile with TI=50% underestimated the LFL distance. The reason for the better prediction with the lower TI in the counter-flow configuration contrast to the co-flow is not clear yet.

The predicted radial profiles of volume fraction up to 2 m from the nozzle were in close agreement with the experiment in all configurations with a tendency to predict a slightly wider cloud.

Finally, experiments and simulations showed that both co-flow and counter-flow configuration lead to reduction of the LFL distance compared to no ventilation. This is attributed to the better mixing and dilution of the cloud. However, to reproduce this behavior in simulations, either high turbulence should be imposed or approaches with non-uniform velocity field across inflow boundary should be applied to mimic the fan flow and to better calculate the flow field generated by the fan.

6.0 ACKNOWLEDGMENTS

The research leading to these results was financially supported by the HyTunnel-CS which has received funding from the Fuel Cells and Hydrogen 2 Joint Undertaking under grant agreement No 826193. This Joint Undertaking receives support from the European Union's Horizon 2020 research and innovation programme, Hydrogen Europe and Hydrogen Europe research.

Numerical simulations conducted in this research by Ulster University were supported via the project Kelvin-2 funded by Engineering and Physical Science Council (EPSRC) U.K. (EPSRC grant number EP/T022175/1).

REFERENCES

1. J. Grune, K. Sempert, M. Kuznetsov, T. Jordan, "Hydrogen jet structure in presence of forced co-, counter- and cross-flow ventilation," in International Conference on Hydrogen Safety, Edinburgh, UK, September 21-23, 2021, paper submitted.
2. E. Papanikolaou and D. Baraldi, "Evaluation of notional nozzle approaches for CFD simulations of free-shear under-expanded hydrogen jets," Int. J. Hydrogen Energy, vol. 37, pp. 18563–18574, 2012.
3. A. G. Venetsanos and S. G. Giannissi, "Release and dispersion modeling of cryogenic under-expanded hydrogen jets," Int. J. Hydrogen Energy, vol. 42, no. 11, pp. 7672–7682, Sep. 2017.
4. V. V. Molkov, Fundamentals of hydrogen safety engineering. www.bookboon.com, 2012.
5. X. Li, D. M. Christopher, E. S. Hecht, and I. W. Ekoto, "Comparison of two-layer model for high pressure hydrogen jets with notional nozzle model predictions and experimental data," in 5th International Conference on Hydrogen Safety, Yokohama,Japan, 2015.
6. V. M. Domkundwar, V. Sriramulu, and M. C. Gupta, "Turbulence Measurements in Swirling Flows.," Def. Sci. J., vol. 31, no. 4, pp. 261–275, 1981.
7. S. K. Halloran, A. S. Wexler, and W. D. Ristenpart, "Turbulent dispersion via fan-generated flows," Phys. Fluids, vol. 26, no. 5, 2014.
8. HyTunnel-D2.2, "Intermediate report on analytical, numerical and experimental studies," 2020.
9. A. D. Birch, D. R. Brown, M. G. Dodson, and F. Swaffield, "The Structure and Concentration Decay of High Pressure Jets of Natural Gas," Combust. Sci. Technol., vol. 36, no. 5–6, pp. 249–261, Apr. 1984.
10. H. Versteeg and W. Malalasekera, An introduction to computational fluid dynamics: the finite volume method. 2007.
11. A. G. Venetsanos, E. Papanikolaou, and J. G. Bartzis, "The ADREA-HF CFD code for consequence assessment of hydrogen applications," Int. J. Hydrogen Energy, vol. 35, no. 8, pp. 3908–3918, Apr. 2010.
12. B. E. Launder and D. B. Spalding, Lectures in Mathematical Models of Turbulence. Academic Press Inc, 1972.
13. I. K. Kikoin, "Tables of Physical Properties," Handbook, Moscow, At., pp. 1006, (in Russian), 1976.